

## ORIGINAL ARTICLE

# Chiroptical properties of cholesteric liquid crystals of chitosan phenylcarbamate in ionic liquids

Junichi Sato, Nobuhiro Morioka, Yoshikuni Teramoto and Yoshiyuki Nishio

Chitosan phenylcarbamate (CtsPC) samples were synthesized with different degrees of substitution (DS) ranging from 2.3 to 3.5, and their lyotropic liquid crystallinity in ionic liquids was investigated. 1-Ethyl-3-methylimidazolium dicyanamide ([C2Mim][N(CN)<sub>2</sub>]) was found to be a novel solvent for CtsPC, and the concentrated lyotropic system formed a cholesteric liquid-crystalline phase and mostly exhibited vivid colorations owing to selective reflection of visible light. Ultraviolet–visible–near-infrared spectroscopy and wide-angle X-ray diffractometry were used to evaluate the maximum wavelength of selective light reflection and the distance and rotational difference between adjacent nematic thin layers in the cholesteric mesophase, respectively. The cholesteric helical pitch increased with decreasing polymer concentration, increasing temperature or increasing DS. The helical sense remained right-handed under the adopted measurement conditions, although CtsPCs are known to form a left-handed cholesteric structure in polar organic solvents, such as *N,N*-dimethylformamide (DMF). Accordingly, an inversion of the cholesteric sense was achieved by combination of [C2Mim][N(CN)<sub>2</sub>] and DMF as solvent; circular dichroism and optical rotatory dispersion spectroscopy verified that the sense of CtsPC cholesterics changed from left-handed to right-handed with increasing [C2Mim][N(CN)<sub>2</sub>] content in the mixed solvent.

*Polymer Journal* (2014) 46, 559–567; doi:10.1038/pj.2014.34; published online 21 May 2014

**Keywords:** chiroptical property; chitosan; ionic liquid; liquid crystal; phenylcarbamate

## INTRODUCTION

A large number of cellulose derivatives, such as polymers and even cellulose microfibrils (nanocrystallites), are capable of forming an optically anisotropic mesophase in various solvents because of the inherent semirigidity and chirality in the carbohydrate backbone.<sup>1–3</sup> The supramolecular structure in the mesophase is usually of a cholesteric (or chiral nematic) type, with possible exceptions such as a columnar type found for thermotropic cellulose trialkanoates.<sup>4</sup> Although there remain unresolved problems concerning the correlation between their molecular structure and the liquid-crystalline phase structure, the general features of the mesomorphic assembly of cellulose derivatives seem to be firmly established.<sup>1–6</sup> In lyotropic systems, for example, the optical properties are significantly affected by the solvent and its composition. (Hydroxypropyl)cellulose liquid crystals in water are colored, but the coloration is markedly changed by the addition of a small amount of inorganic salts or organoionic liquids (ILs) (imidazolium salts) as the third component.<sup>7,8</sup> As another example, several ILs can be a direct solvent for chemically unmodified cellulose, and the use of 1-butyl-3-methylimidazolium chloride in particular leads to a viscous cellulose solution that can display optical birefringence at polymer concentrations of more than 10 wt%.<sup>9</sup>

Meanwhile, chitin and chitosan are the second most abundant polysaccharides after cellulose, widely distributed in the crusts of

marine crustaceans, as well as in the exoskeletons of many species of insects. These two polysaccharides are structurally similar to cellulose; chitin consists of 2-acetamido-2-deoxy- $\beta$ -D-glucose units through a  $\beta$ (1 $\rightarrow$ 4) linkage, and chitosan is an *N*-deacetylated derivative of chitin. In contrast to the situation of cellulose derivatives, there have been few studies on the liquid-crystalline behavior of chitin or chitosan derivatives,<sup>10–13</sup> except for the mesophase characterization of chitin nanocrystals (microfibrils).<sup>14,15</sup> As one of these examples, we reported the molecular structure and liquid-crystalline characteristics of chitosan phenylcarbamate (CtsPC; Figure 1a) in polar organic solvents such as *N,N*-dimethylformamide (DMF), *N,N*-dimethylacetamide (DMAc) and dimethyl sulfoxide;<sup>16</sup> CtsPC was found to form a left-handed cholesteric arrangement, irrespective of variations in temperature, polymer concentration, degrees of substitution (DS) and the solvent species used.

There have been a few recent studies on the dissolution of chitin in ILs, in which 1-butyl-3-methylimidazolium chloride,<sup>17</sup> 1-ethyl-3-methylimidazolium chloride<sup>18</sup> and 1-butyl-3-methylimidazolium acetate<sup>19</sup> were reported to be good solvents. Such ILs have attracted a great deal of attention not only as green solvent media but also as electrolytes in ion-conductive materials.<sup>20</sup> For instance, anisotropic ion conductivity has been accomplished in liquid-crystalline layered assemblies consisting of a pair of IL/mesogenic molecules of modest molecular weight.<sup>21</sup> As for polysaccharide derivatives, investigations

into the thermotropic liquid crystallinity and ion conductivity of a cellulose derivative with dangling poly(ethylene oxide) side-chains have been pursued.<sup>22</sup> Moreover, a lithium ion battery made up of a polymer gel of cellulose derivative/poly(ethylene glycol) dimethacrylate has been reported to show a practical level of ionic conductivity.<sup>23</sup> These examples raise the possibility that ILs could serve as direct solvents for lyotropic liquid crystals of polysaccharide derivatives and that such lyotropics should be used as novel devices responding to external stimuli (including light and electric field). To our knowledge, however, no work has been reported on the explicit liquid-crystalline phase behavior and related functionalities of chitin or chitosan derivatives in ILs as specific fluid media.

In the present study, we examined a series of CtsPC samples for distinct observation of mesophase formation in imidazolium salts. In continuation of our study on the molecular modification and liquid crystallinity of chitosan, we aimed to elucidate the possible cholesteric ordering and ensuing optical properties of CtsPC lyotropics in relation to molecular parameters such as DS, as well as the surrounding conditions, including polymer concentration, temperature and solvent composition.

## EXPERIMENTAL PROCEDURE

### Materials

Chitosan materials, lot HF-1 ( $M_v = 1.06 \times 10^5$ ) and HC-2W ( $M_v = 1.46 \times 10^5$ ) of Hokkaido Soda (Hokkaido, Japan), were used after a regeneration treatment.<sup>16</sup> Phenyl isocyanate, DMAc, 1-methylimidazole, iodoethane, lithium bis(trifluoromethanesulfonyl)imide, silver nitrate and ethyl acetate were purchased from Wako Pure Chemical Industries (Osaka, Japan), and used as received. Ethyl bromide, 1-bromobutane, 1-allyl chloride, DMF, toluene and methanol were purchased from Nacalai Tesque (Kyoto, Japan) and used without further purification. 1-Chlorobutane and 1-bromohexane were purchased from Sigma-Aldrich (Tokyo, Japan), and used as supplied. Commercially available potassium hexafluorophosphate (Tokyo Chemical Industry, Tokyo, Japan) and sodium dicyanamide (Alfa Aesar GmbH, Karlsruhe, Germany) were used as received.

### Measurements

An ultraviolet-visible-near-infrared (UV-Vis-NIR) spectrometer (HITACHI U-4100, Hitachi High-Technologies Corporation, Tokyo, Japan) equipped with a thermoregulated cell holder was used to determine selective light-reflection bands. Circular dichroism (CD) and optical rotatory dispersion measurements were conducted with a Jasco J-820DH spectropolarimeter (JASCO Corporation, Tokyo, Japan) to examine the handedness of the cholesteric helical structure. CD spectra were also utilized to determine the selective light-reflection bands in the case where the corresponding signal in UV-Vis-NIR spectra was too small to detect the maximum reflective wavelength. An Olympus polarized optical microscope (POM) (BX60F5, Olympus Corporation, Tokyo, Japan) was used to verify the optical anisotropy of concentrated solutions and observe a fingerprint pattern for cholesteric liquid crystals with relatively long pitch. Refractive index measurements were carried out using an Abbé refractometer (Atago Co., Ltd. (Tokyo, Japan) Type 2T) equipped with a thermoregulated stage and polarizer rotatable over the eyepiece.

The distance and angular difference of rotation between adjacent thin layers in the cholesteric structure were estimated with the aid of wide-angle X-ray diffractometry. The wide-angle X-ray diffractometry measurements were carried out at 25 °C using a Rigaku Ultima IV (Rigaku, Osaka, Japan) in reflection mode. Nickel-filtered Cu K $\alpha$  radiation was used at 40 kV and 40 mA. Fluid samples were relaxed for at least 24 h in a copper sample holder of 0.5 mm height, and diffraction intensity profiles were subsequently collected in a range of  $2\theta = 3 - 20^\circ$ .

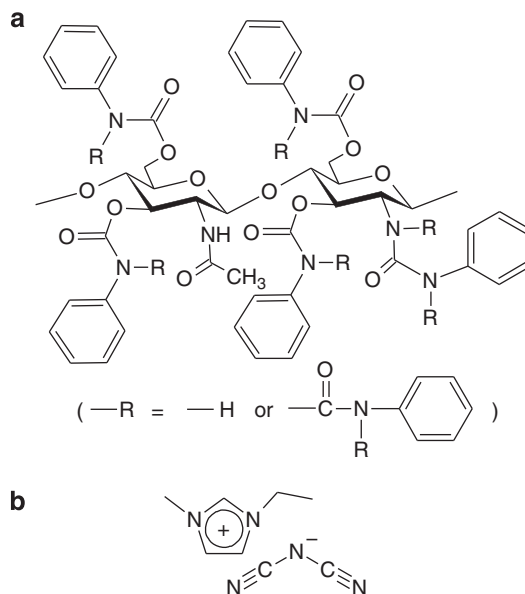


**Figure 1** Structural formulae of (a) chitosan phenylcarbamate (CtsPC) and (b) 1-ethyl-3-methylimidazolium dicyanamide ([C2Mim][N(CN)<sub>2</sub>]).

### Synthesis and characterization of CtsPC

The procedure for synthesis and characterization of CtsPC was almost identical to that described elsewhere.<sup>16</sup> In brief, phenyl isocyanate (7.5–15 equiv per glucosamine unit) was added to a chitosan/DMAc suspension (polymer conc., 3 wt%) in a flask under a dry N<sub>2</sub> atmosphere. The reactive system was continuously stirred at 25 °C in the closed vessel for a prescribed time period (72–144 h). The resulting homogeneous solution was added dropwise into a vigorously stirred, large excess amount of methanol. Each product obtained as a precipitate was filtered and purified with DMF and methanol. The purified CtsPC was treated by Soxhlet extraction with methanol for 1 week to thoroughly remove DMF and dried at 40 °C *in vacuo* for 48 h. Substitution parameters of the CtsPC products were evaluated by proton nuclear magnetic resonance (<sup>1</sup>H NMR) spectroscopy.

### Synthesis of ILs

All the *N*-substituted imidazolium salts used were synthesized through *N*-alkylation/quaternization of 1-methylimidazole with different alkyl halides or allyl halide and subsequent anion exchange if necessary, by reference to the literature.<sup>24–28</sup> For instance, the procedure to obtain 1-ethyl-3-methylimidazolium dicyanamide ([C2Mim][N(CN)<sub>2</sub>]; Figure 1b) was as follows: 1-methylimidazole (0.10 mol) was stirred at room temperature in a round-bottomed flask equipped with a reflux condenser under a dry N<sub>2</sub> atmosphere, and iodoethane (0.15 mol) was added at adequate time intervals. After the mixture was stirred at 70 °C for 18 h, the upper phase containing unreacted reagents was decanted. The residual crude product was lightly washed with hot toluene and then thoroughly with ethyl acetate by the combined use of stirring and ultrasonic treatment. After decanting ethyl acetate, the remaining solvent was removed by heating the IL phase to 70 °C and stirring while on a vacuum line. The resultant 1-ethyl-3-methylimidazolium iodide (0.10 mol) was once dissolved in a small quantity of distilled water, and then the salt solution was mixed with silver dicyanamide (0.11 mol) that was previously prepared by mixing equimolar amounts of silver nitrate and sodium dicyanamide. After vigorous stirring at 40 °C over 5 h, the objective product [C2Mim][N(CN)<sub>2</sub>] was purified by filtration and drying *in vacuo* at 60 °C for 48 h. In an essentially similar manner, 1-butyl-3-methylimidazolium chloride ([C4Mim][Cl]), 1-butyl-3-methylimidazolium bromide ([C4Mim][Br]), 1-hexyl-3-methylimidazolium bromide ([C6Mim][Br]), 1-allyl-3-methylimidazolium chloride ([AMim][Cl]), 1-ethyl-3-methylimidazolium bis(trifluoromethanesulfonyl)imide ([C2Mim][Tf<sub>2</sub>N]), 1-butyl-3-methylimidazolium

bis(trifluoromethanesulfonyl)imide ([C4Mim][Tf<sub>2</sub>N]) and 1-butyl-3-methylimidazolium hexafluorophosphate ([C4Mim][PF<sub>6</sub>]) were synthesized with the relevant reagents. The salt products were all identified as the respective objects of *N*-substituted methylimidazolium salts by <sup>1</sup>H NMR measurements (see Supplementary Information) and elemental analysis. The elemental analysis was conducted only to confirm the absence of halogen and thus completion of anion exchange.

### Preparation of CtsPC/IL solutions

CtsPC solutions were prepared in a polymer concentration range of 5–45 wt% by using the ILs described above. The prescribed amount of solvent was added to CtsPC powder weighed in a hermetically sealable glass vial and placed at 25 °C over a period of 3 months. In the procedure, the vial was turned upside down and centrifuged at intervals for the purpose of accelerating the dissolution of CtsPC.

A separate series of CtsPC solutions was also prepared at 46 wt% by using a mixed solvent (MxS) consisting of [C2Mim][N(CN)<sub>2</sub>] and DMF, according to the above technique.

## RESULTS AND DISCUSSION

### Substitution parameters of CtsPC

<sup>1</sup>H NMR data were used for determination of the values of DS, MS (molar substitution) and degree of polymerization in the side chains of CtsPC, where DS and MS denote the average number of phenylcarbamoyl substitution associated with the four protons of C2–NH<sub>2</sub>, C3–OH and C6–OH and that of all phenylcarbamoyl entities introduced, respectively, per glucosamine residue of chitosan, and degree of polymerization in the side chains is defined as the average degree of phenylcarbamoyl polyaddition for the modified sites of a possible four.<sup>16</sup> The structural parameters evaluated for the CtsPC samples are summarized in Table 1, where CtsPC of DS = *x* is encoded as CtsPC<sub>*x*</sub>.

### Solubility of CtsPC in ILs

Table 2 shows the solubility of CtsPC<sub>2.84</sub> as a representative CtsPC product in each IL solvent at room temperature (25 °C). CtsPC was soluble in [C4Mim][Cl], [C4Mim][Br] and [C6Mim][Br], and provided an isotropic phase in the polymer concentration range of 5–10 wt%. When the concentration was elevated to 15 or 20 wt%, the three lyotropics all transformed into a gelatinous state, although optical birefringence was noted in the CtsPC/[C4Mim][Br] system. In the use of [AMim][Cl], [C2Mim][Tf<sub>2</sub>N], [C4Mim][Tf<sub>2</sub>N] and [C4Mim][PF<sub>6</sub>], CtsPC was insoluble in each, even at low concentrations such as 5 wt%. In [C2Mim][N(CN)<sub>2</sub>], surprisingly, CtsPC formed an anisotropic phase at polymer concentrations exceeding 15 wt% and dissolved even at a higher concentration of 45 wt% so

that the solution exhibited a vivid cholesteric color. It was thus revealed that the solubility of CtsPC was significantly affected by anion species of ILs rather than the side-chain structure (such as alkyl chain length) of imidazolium cations.

### Helical pitch of CtsPC/[C2Mim][N(CN)<sub>2</sub>] cholesterics

Optical properties of cholesteric liquid crystals are mainly governed by the periodicity in the supramolecular helical structure. For the present CtsPC lyotropic system, the practically important cholesteric pitch (*P*) was evaluated for the explicit dependence on three variable factors: polymer concentration, temperature and DS. The wavelength ( $\lambda_M$ ) that gives a peak maximum of a reflection band can be related to the cholesteric pitch by the de Vries equation:<sup>29</sup>

$$\lambda_M = \bar{n}P \quad (1)$$

where  $\bar{n}$  is an average refractive index of the mesophase. For all the CtsPC/[C2Mim][N(CN)<sub>2</sub>] samples explored in this paper, the index  $\bar{n}$  decreased with increasing temperature and with decreasing polymer concentration; nevertheless, the two variables did not greatly affect the second decimal place of the  $\bar{n}$  data. In addition, the values of  $\bar{n}$  were only slightly scattered by DS variation (2.35–3.51). For the calculation of *P* by Equation (1), therefore, it was substantially sufficient to adopt  $\bar{n} = 1.54$ , fitting the value of 1.540 obtained for a 40 wt% CtsPC<sub>2.84</sub>/[C2Mim][N(CN)<sub>2</sub>] solution at 25 °C.

Figure 2 illustrates selective light-reflection spectra obtained for the 40 wt% CtsPC<sub>2.84</sub>/[C2Mim][N(CN)<sub>2</sub>] solution at different temperatures under the usual condition of the incident light beam being normal to the planar cholesteric phase. These spectra serve as a typical example that demonstrates a systematic red shift in  $\lambda_M$  of the selective light reflection, accompanied by suppression in peak intensity, with an elevation in temperature; at  $\geq 70$  °C, the reflectance became too small to be detected. A similar spectral transformation upon heating was observed for all cholesteric solutions explored, differing in degree but not in direction of peak shift. As for kinetics, the concentrated solutions (0.2 g, encapsulated in a cylinder-shaped vial) relatively slowly responded to thermal stimuli, viz. complete shift of the coloration was observed  $\sim 10$  min after temperature change. Therefore, temperature-variable optical measurements were conducted following 30-min relaxation treatment to realize sufficient color shift.

Figure 3a shows the relation between *P* and temperature for CtsPC<sub>2.72</sub>/[C2Mim][N(CN)<sub>2</sub>] and CtsPC<sub>2.84</sub>/[C2Mim][N(CN)<sub>2</sub>]

**Table 1** Starting material and substitution parameters for CtsPC samples

sample code	Starting material	DS	MS	DP <sub>s</sub>
CtsPC <sub>2.35</sub>	HC-2W	2.35	2.41	1.02
CtsPC <sub>2.47</sub>	HC-2W	2.47	2.76	1.12
CtsPC <sub>2.72</sub>	HC-2W	2.72	2.99	1.10
CtsPC <sub>2.84</sub>	HF-1	2.84	3.01	1.06
CtsPC <sub>2.94</sub>	HF-1	2.94	3.04	1.03
CtsPC <sub>3.02</sub>	HC-2W	3.02	3.17	1.05
CtsPC <sub>3.05</sub>	HF-1	3.05	3.29	1.08
CtsPC <sub>3.51</sub>	HF-1	3.51	3.83	1.09

Abbreviations: CtsPC, chitosan phenylcarbamate; DP<sub>s</sub>, degree of polymerization in the side chains; DS, degrees of substitution; MS, molar substitution.

**Table 2** Solubility of CtsPC<sub>2.84</sub> in various ionic liquids at 25 °C

Ionic liquid	Polymer conc. (wt%)					
	5	10	15	20	30	45
[C4Mim][Cl]	I	I	G	–	–	–
[C4Mim][Br]	I	I	A	G	–	–
[C6Mim][Br]	I	I	G	–	–	–
[AMim][Cl]	×	×	–	–	–	–
[C2Mim][Tf <sub>2</sub> N]	×	×	–	–	–	–
[C4Mim][Tf <sub>2</sub> N]	×	×	–	–	–	–
[C4Mim][PF <sub>6</sub> ]	×	×	–	–	–	–
[C2Mim][N(CN) <sub>2</sub> ]	I	I	A	A	C	C

Abbreviations: A, anisotropic; [AMim][Cl], 1-allyl-3-methylimidazolium chloride; C, cholesteric; [C2Mim][N(CN)<sub>2</sub>], 1-ethyl-3-methylimidazolium dicyanamide; [C4Mim][Cl], 1-butyl-3-methylimidazolium chloride; [C4Mim][Br], 1-butyl-3-methylimidazolium bromide; [C6Mim][Br], 1-hexyl-3-methylimidazolium bromide; [C4Mim][PF<sub>6</sub>], 1-butyl-3-methylimidazolium hexafluorophosphate; [C2Mim][Tf<sub>2</sub>N], 1-ethyl-3-methylimidazolium bis(trifluoromethanesulfonyl)imide; [C4Mim][Tf<sub>2</sub>N], 1-butyl-3-methylimidazolium bis(trifluoromethanesulfonyl)imide; G, gelatinous; I, isotropic; ×, insoluble; –, not prepared.

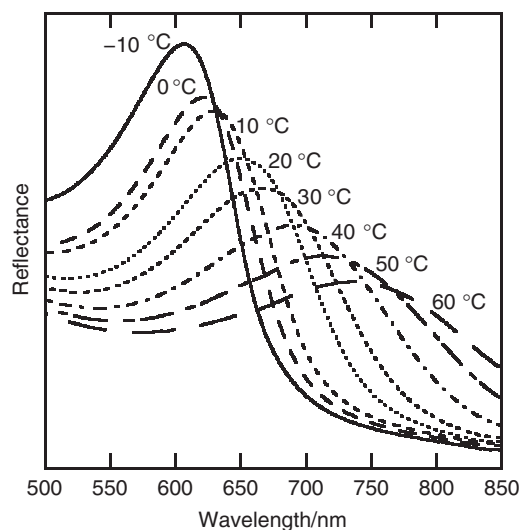


**Figure 2** Selective light reflection spectra obtained for a 40 wt% CtsPC<sub>2.84</sub>/[C2Mim][N(CN)<sub>2</sub>] solution at different temperatures. [C2Mim][N(CN)<sub>2</sub>], 1-ethyl-3-methylimidazolium dicyanamide; CtsPC, chitosan phenylcarbamate.

solutions prepared at a fixed polymer concentration of 40 wt%. We observe that the respective cholesteric pitches monotonically increase with elevating temperature in the limits possible for measuring the data point. This temperature dependence of cholesteric pitch will be interpreted below, in relation to the short-range order (interlayer distance and twist angle) of the cholesteric architecture. Herein, as a general trend,  $P$  of the CtsPC lyotropics of  $DS = 2.7\text{--}3.0$  increased with temperature at a much higher rate than in situations involving other CtsPC series of  $DS < 2.7$  or  $DS > 3.0$ . In accordance with the higher sensitivity of  $P$  referring to the former class, visually, the CtsPC<sub>2.72</sub>/[C2Mim][N(CN)<sub>2</sub>] solution was greenish at  $-10\text{ }^\circ\text{C}$ , turned orange-colored or yellowish as the temperature was raised to  $60\text{ }^\circ\text{C}$  and, ultimately, became uncolored at  $70\text{ }^\circ\text{C}$ . The CtsPC<sub>2.84</sub>/[C2Mim][N(CN)<sub>2</sub>] solution was generally reddish in the temperature range of  $-10$  to  $60\text{ }^\circ\text{C}$ , but the hue became quite profound with increasing temperature and, at  $70\text{ }^\circ\text{C}$ , the sample was totally uncolored. However, the two solutions were still anisotropic right after discoloring at  $70\text{ }^\circ\text{C}$  and became isotropic directly at  $90\text{ }^\circ\text{C}$ , which was confirmed by POM observation. The discoloration and isotropic transition points both tended to shift upward when the polymer concentration was raised. As summarized below, the cholesteric helical sense was always right-handed, as the CtsPC solutions retained this type of mesophase below the individual isotropic transition temperature.

Figure 3b embodies the concentration dependence of cholesteric pitch for the CtsPC<sub>2.72</sub>/[C2Mim][N(CN)<sub>2</sub>] and CtsPC<sub>2.84</sub>/[C2Mim][N(CN)<sub>2</sub>] series at  $25\text{ }^\circ\text{C}$ . In both series, the pitch decreased almost linearly in proportion to CtsPC concentration. The negative correlation between pitch and concentration seems to be a natural phenomenon, taking into consideration the increase in relative density of the solute polymer in the cholesteric mesophase; however, caution should be exercised in this interpretation because the opposite case (positive correlation) is actually known, for instance, for a lyotropic system of cellulose triphenylcarbamate/diethylene glycol monoethyl ether.<sup>5</sup> In this context, the concentration dependence of the short-range order in the CtsPC/[C2Mim][N(CN)<sub>2</sub>] cholesterics is investigated in the next section.

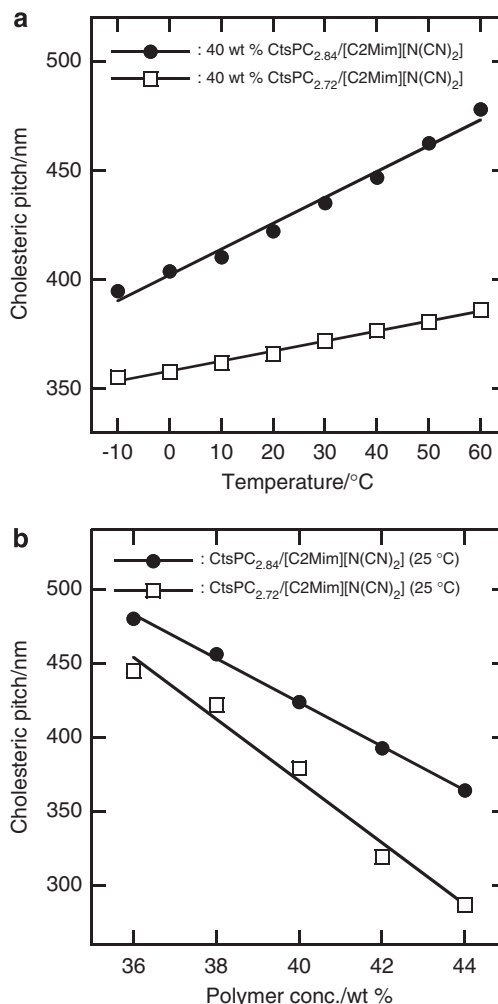
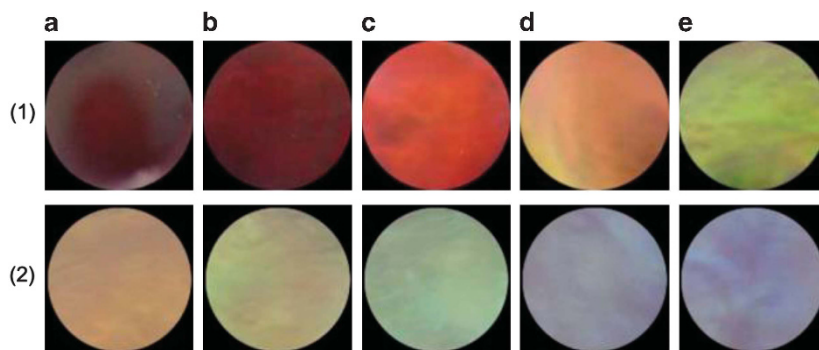


**Figure 3** Cholesteric pitch for CtsPC<sub>2.84</sub>/[C2Mim][N(CN)<sub>2</sub>] and CtsPC<sub>2.72</sub>/[C2Mim][N(CN)<sub>2</sub>] series: (a) temperature dependence at a fixed polymer concentration of 40 wt%; (b) polymer concentration dependence at a constant temperature of  $25\text{ }^\circ\text{C}$ . [C2Mim][N(CN)<sub>2</sub>], 1-ethyl-3-methylimidazolium dicyanamide; CtsPC, chitosan phenylcarbamate.

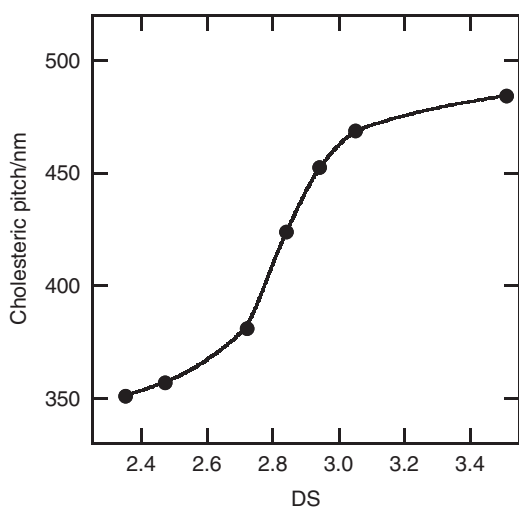
In the use of the CtsPC products of  $DS = 2.7\text{--}3.0$ , the reflective coloration of the cholesteric solutions had a stronger monochromaticity and was sensitive to the concentration change, *viz.*, the vivid color moved quite sharply from the red side to blue side in the spectral array as the polymer concentration increased (Figure 4). This result most likely occurs because  $DS \approx 2.8$  ( $MS \approx 3.0$ ) is the optimum substitution for CtsPC to form a well-ordered cholesteric mesophase in terms of molecular structure; simultaneously, the helical assembly of such a CtsPC is highly responsive in periodicity to a small fluctuation of surrounding conditions, including temperature and solvent concentration.

Figure 5 exemplifies the  $DS$  dependence of cholesteric pitch for 40 wt% CtsPC/[C2Mim][N(CN)<sub>2</sub>] samples at  $25\text{ }^\circ\text{C}$ . As observed from the plot, the increase in  $DS$  from 2.35 to 3.51 leads to a marked rise in  $P$ , the overall increment being more than 130 nm. The steepest increase of  $P$  is observed at around  $DS = 2.8$ , followed by saturation in the higher  $DS$  range of  $\geq 3.0$ . This example indicates that the supramolecular helicoid of CtsPC of  $DS \approx 2.8$  is also sensitive in twisting power to a small fluctuation of  $DS$  itself. In association with





**Figure 4** Photographs showing cholesteric colors for solutions of (1) CtsPC<sub>2.84</sub> and (2) CtsPC<sub>2.72</sub> in [C2Mim][N(CN)<sub>2</sub>]. Polymer concentration: (a) 36 (b) 38, (c) 40, (d) 42 and (e) 44 wt%. All photographs were obtained through digital scanning of the bottom of each individual sample vial at 25 °C. [C2Mim][N(CN)<sub>2</sub>], 1-ethyl-3-methylimidazolium dicyanamide; CtsPC, chitosan phenylcarbamate.



**Figure 5** Degrees of substitution (DS) dependence of cholesteric pitch for 40 wt% CtsPC/[C2Mim][N(CN)<sub>2</sub>] solutions at 25 °C. [C2Mim][N(CN)<sub>2</sub>], 1-ethyl-3-methylimidazolium dicyanamide; CtsPC, chitosan phenylcarbamate.

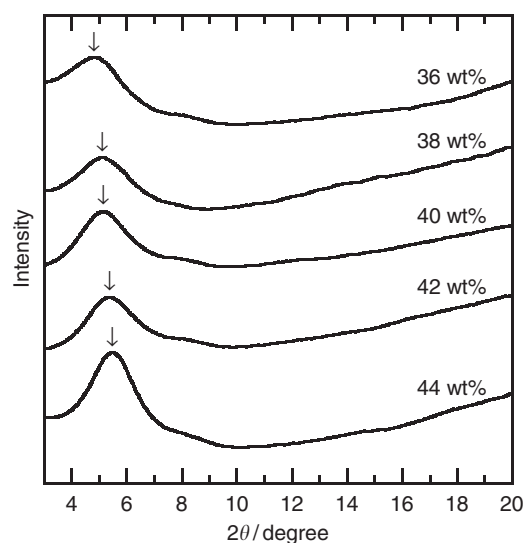


**Figure 6** Wide-angle X-ray diffractometry (WAXD) intensity profiles obtained for 36–44 wt% CtsPC<sub>2.84</sub>/[C2Mim][N(CN)<sub>2</sub>] solutions at 25 °C. [C2Mim][N(CN)<sub>2</sub>], 1-ethyl-3-methylimidazolium dicyanamide; CtsPC, chitosan phenylcarbamate.

this pitch–DS relation, DS dependence of the short-range ordering in the cholesterics is discussed below.

#### Short-range order in mesophase of CtsPC/[C2Mim][N(CN)<sub>2</sub>]

Figure 6 illustrates wide-angle X-ray diffractometry intensity profiles measured for CtsPC<sub>2.84</sub>/[C2Mim][N(CN)<sub>2</sub>] cholesterics of 36–44 wt% at 25 °C. All diffraction intensity curves gave only one significant peak at a lower angular position of  $2\theta = 5.0\text{--}5.5^\circ$ , except for a diffuse scattering halo centered at  $2\theta \approx 20^\circ$ . Therefore, the CtsPC/[C2Mim][N(CN)<sub>2</sub>] solutions are found to assume an essentially nematic structure, and the short-range ordering of less than a few nanometers in the mesophase is analyzable in terms of a pseudohexagonal packing of the molecular chains. The distance ( $d$ ) between the nematic layers stacking in the mesophase can thus be directly estimated from the low-angle peak. The following values were estimated by Bragg's equation ( $\lambda = 2d \sin \theta$ ,  $\lambda = 0.1542 \text{ nm}$ ) for the five samples given in Figure 6:  $d = 1.80, 1.73, 1.71, 1.65$  and  $1.61 \text{ nm}$ , decreasing gradually with increasing CtsPC concentration (Figure 7a). The temperature dependence of  $d$  was also evaluated for the 40 wt% CtsPC<sub>2.84</sub>/[C2Mim][N(CN)<sub>2</sub>] sample; the  $d$  value slightly fluctuated from 1.71 to 1.72 nm with increasing temperature from 25 to 60 °C (Figure 7b). Moreover, the DS dependence of  $d$  was examined at

25 °C for 40 wt% solutions of various CtsPC products in [C2Mim][N(CN)<sub>2</sub>]; the distance increased slightly from 1.66 to 1.72 nm with an increase in DS from 2.35 to 3.51 (Figure 7c). To sum up by comparison,  $d$  depended on CtsPC concentration to an appreciable extent but was hardly affected by temperature or DS.

Subsequently, the cholesteric twist angle ( $\varphi$ ), defined as an azimuth difference between adjacent nematic thin layers, was calculated from the relation  $\varphi = 360^\circ d/P$  by additional use of the cholesteric pitch data obtained in optical measurements. In the CtsPC<sub>2.84</sub>/[C2Mim][N(CN)<sub>2</sub>] lyotropics at 25 °C (Figure 7a), the value of  $\varphi$  increased almost linearly from 1.35 to 1.59° with increasing CtsPC concentration (36–44 wt%). Considering the diminution in  $d$  commensurate to the concentration increment, we ultimately find that the decrease in layer spacing and increase in twist angle, each accompanying the concentration increase, are both responsible for the negative concentration dependence of cholesteric pitch. In Figure 7b, the variation of  $\varphi$  with temperature is estimated for the 40 wt% CtsPC<sub>2.84</sub>/[C2Mim][N(CN)<sub>2</sub>] solution; the value decreased linearly from 1.45° to 1.30° with increasing temperature from 25 to 60 °C. As layer spacing  $d$  was hardly affected by temperature elevation, it can

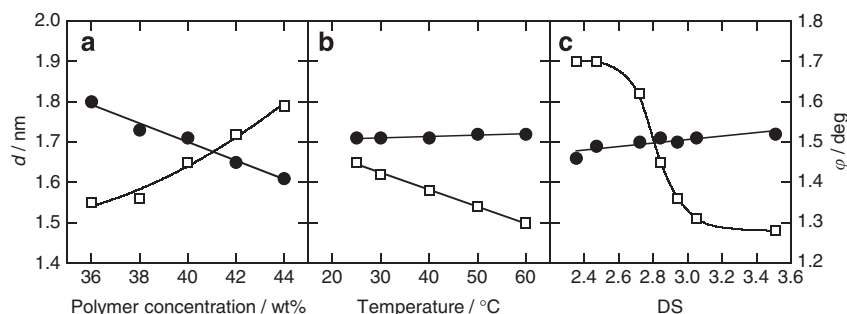


**Figure 7** Plots of the interlayer distance  $d$  (filled circle) and twist angle  $\varphi$  (open square) for CtsPC/[C2Mim][N(CN)<sub>2</sub>] lyotropics, constructed as a function of three variables: (a) polymer concentration (at 25 °C and degrees of substitution (DS) = 2.84); (b) temperature (at 40 wt% polymer and DS = 2.84); (c) DS of CtsPC (at 25 °C and 40 wt% polymer). [C2Mim][N(CN)<sub>2</sub>], 1-ethyl-3-methylimidazolium dicyanamide; CtsPC, chitosan phenylcarbamate.

be deduced that the correlation of  $P$  with temperature was determined only by the variable twist angle. Lastly, the twist angle was evaluated for the 40 wt% lyotropics of different CtsPCs (DS = 2.35–3.51) in [C2Mim][N(CN)<sub>2</sub>] (25 °C), and the resulting values (1.70–1.28°) are plotted in Figure 7c. In this plot, the steepest decrease of  $\varphi$  with increasing DS occurs at DS  $\approx$  2.8, whereas the slopes in the ranges of DS < 2.6 and of DS > 3.0 are quite gentle. However, the increment in  $d$  caused by DS elevation was, substantially, negligibly small; hence, the distinctive variation of  $P$  shown in Figure 5 is attributable to the variation of  $\varphi$ . The cholesteric interlayer interaction, possibly associated with a chiral conformation (helical or twisted form) of the constituent CtsPC chains, would change in strength, sensitively responding to the DS variation between 2.6 and 3.0. As a natural assumption, the sharp response of  $P$  to surrounding conditions observed for the CtsPC products of DS = 2.7–3.0 can also be ascribed to the definitive  $\varphi$ –DS correlativity.

#### Handedness of cholesteric mesophase

CD spectroscopy is a useful tool, providing information about both the pitch and rotational sense specifying a cholesteric helix. In the present measurements, most of the observed CD signals were so large that the tops of their peaks were often out of the measurable range, even when the sample thickness was reduced to 100  $\mu$ m. Therefore, those spectra were used principally to determine the handedness of the cholesteric helical structure. As a result, all lyotropics of the CtsPC products in [C2Mim][N(CN)<sub>2</sub>] gave a ‘negative’ pseudo-Cotton effect in the wavelength range of the selective light reflection, irrespective of variations in temperature (–10 to 60 °C), polymer concentration (30–45 wt%) and DS (2.35–3.51), which is in sharp contrast to the ‘positive’ effect observed with the use of polar aprotic solvents.<sup>16</sup> It was thus verified that we realized a ‘right-handed’ cholesteric arrangement for the chitin/chitosan-based derivative. However, it is difficult from the above experiments to clarify the reason for the dependence of cholesteric helical sense changes on solvent species, due to the lack of lucid data linking conformation of the polysaccharide molecules directly to their chiral liquid-crystalline structure. As far as the authors can infer, it may be possible that the electric dipole moments of solvents affect that of the urethane-linked phenylcarbamoyl substituents, leading to the alteration of some secondary structure of CtsPC molecules and also the inverse of cholesteric sense.

#### Inversion of cholesteric sense by changing solvent composition

In our previous work,<sup>16</sup> CtsPC lyotropics with a polar aprotic solvent (such as DME, DMAc or dimethyl sulfoxide) always formed a left-handed cholesteric structure. Accordingly, with the possibility of

observing the inversion of cholesteric sense, we prepared new solutions of three CtsPCs (DS = 2.72, 3.02 and 3.51) at a fixed concentration of 46 wt% by using a MxS consisting of [C2Mim][N(CN)<sub>2</sub>] and DMF. Hereinafter, a CtsPC<sub>*x*</sub> solution whose solvent composition is [C2Mim][N(CN)<sub>2</sub>]:DMF =  $n$ :(10 –  $n$ ) in weight is encoded as CtsPC<sub>*x*</sub>/MxS<sub>*n*/(10 – *n*)</sub>. Figure 8 shows the visual appearance of a series of CtsPC<sub>3.02</sub> lyotropics in MxS at 25 °C. The four samples of CtsPC<sub>3.02</sub>/MxS<sub>0/10</sub>, CtsPC<sub>3.02</sub>/MxS<sub>2/8</sub>, CtsPC<sub>3.02</sub>/MxS<sub>8/2</sub> and CtsPC<sub>3.02</sub>/MxS<sub>10/0</sub> imparted vivid reflection colors, whereas such coloration was never perceived for CtsPC<sub>3.02</sub>/MxS<sub>4/6</sub> and CtsPC<sub>3.02</sub>/MxS<sub>6/4</sub>; however, each of the six samples was thoroughly anisotropic in POM observations.

For the CtsPC<sub>3.02</sub>/MxS lyotropics, excluding CtsPC<sub>3.02</sub>/MxS<sub>6/4</sub> only,  $\lambda_M$  was successfully determined by UV–Vis–NIR spectroscopy, covering a range of  $\lambda$  = 300–2500 nm. In refractometry measurements for the lyotropic series (25 °C), the index  $\bar{n}$  increased by 0.01 in proportion as the weight fraction of [C2Mim][N(CN)<sub>2</sub>] in MxS increased by 20%, that is, we obtained  $\bar{n}$  = 1.51, 1.52, ..., 1.56 for CtsPC<sub>3.02</sub>/MxS<sub>0/10</sub>, CtsPC<sub>3.02</sub>/MxS<sub>2/8</sub>, ..., CtsPC<sub>3.02</sub>/MxS<sub>10/0</sub>. Thus, for the five samples concerned, the value of each cholesteric pitch was readily calculable according to Equation (1).

With regard to the remaining sample, CtsPC<sub>3.02</sub>/MxS<sub>6/4</sub>, POM revealed that the anisotropic phase was endowed with a well-developed fingerprint texture in the optical image, as illustrated in Figure 9a. This optical pattern is characteristic of a cholesteric liquid crystal with comparatively longer helical periodicity. The repeating distance ( $S_r$ ) of the so-called retardation lines making up the pattern corresponds to half the cholesteric pitch. From high-magnification POM data (Figure 9b), the average of  $S_r$  was assessed to be  $\sim$  12  $\mu$ m, so that  $P$  of the cholesteric CtsPC<sub>3.02</sub>/MxS<sub>6/4</sub> would approximate 24  $\mu$ m.

Figure 10a displays CD spectra obtained for the CtsPC<sub>3.02</sub> solutions mentioned above. The derivative CtsPC<sub>3.02</sub> formed a left-handed cholesteric mesophase in MxS<sub>0/10</sub> and MxS<sub>2/8</sub> and, in contrast, a right-handed cholesteric mesophase in MxS<sub>8/2</sub> and MxS<sub>10/0</sub>. For the two samples CtsPC<sub>3.02</sub>/MxS<sub>4/6</sub> and CtsPC<sub>3.02</sub>/MxS<sub>6/4</sub>, whose CD signals were too weak to correctly determine the cholesteric sense thereby, optical rotatory dispersion spectra were also measured, as shown in Figure 10b. de Vries formulated the wavelength dependence of optical rotation caused by a cholesteric liquid–crystalline domain in the following manner:<sup>29</sup>

$$\alpha = \pi(\Delta n)^2 P / [4\lambda^2 \{1 - (\lambda/\lambda_M)^2\}] \quad (2)$$

where  $\alpha$  is the optical rotation per unit length for light of wavelength  $\lambda$ ,  $\lambda_M$  is the maximum wavelength of selective light reflection,  $\Delta n$  is the birefringence of a nematic layer as structural constituent and the

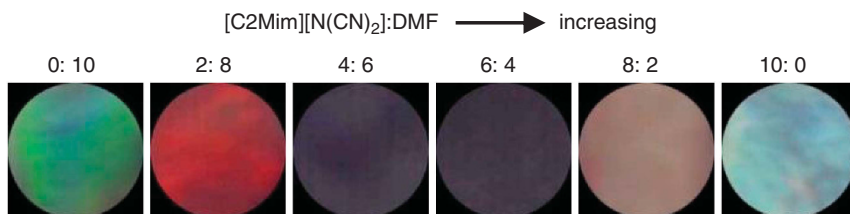


**Figure 8** Photographs showing the visual appearance of a series of 46 wt% CtsPC<sub>3,02</sub>/[C2Mim][N(CN)<sub>2</sub>]/DMF lyotropics at 25 °C. [C2Mim][N(CN)<sub>2</sub>], 1-ethyl-3-methylimidazolium dicyanamide; CtsPC, chitosan phenylcarbamate; DMF, *N,N*-dimethylformamide.

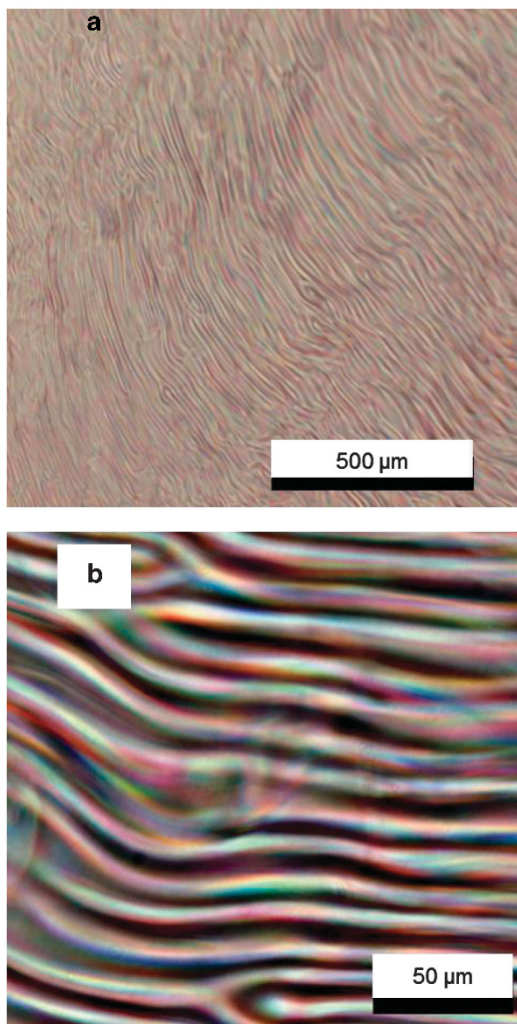


**Figure 9** Polarized optical micrographs of CtsPC<sub>3,02</sub>/MxS<sub>6/4</sub> (46 wt% CtsPC<sub>3,02</sub> solution in 6:4 [C2Mim][N(CN)<sub>2</sub>]/DMF). Scale bars denote 500 μm in (a) or 50 μm in (b). The sample thickness is ~100 μm. [C2Mim][N(CN)<sub>2</sub>], 1-ethyl-3-methylimidazolium dicyanamide; CtsPC, chitosan phenylcarbamate; DMF, *N,N*-dimethylformamide; MxS, mixed solvent.

cholesteric pitch  $P$  here is taken to be a pseudoscalar that is positive for a right-handed helix and negative for a left-handed helix. For the case of  $\lambda/\lambda_M \ll 1$ , the above equation reduces to

$$\alpha \approx \pi(\Delta n)^2 P / 4\lambda^2 \quad (3)$$

Therefore, in the wavelength region of  $\lambda \ll \lambda_M$ , it follows that  $\alpha$  assumes positive or negative values when the cholesteric sense is right

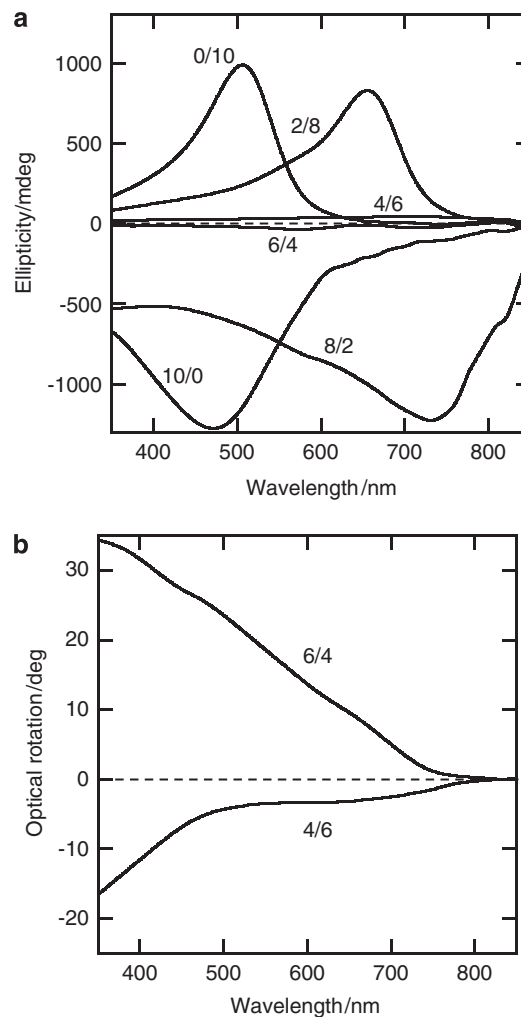


**Figure 10** (a) CD and (b) optical rotatory dispersion (ORD) spectra obtained for the CtsPC<sub>3,02</sub>/[C2Mim][N(CN)<sub>2</sub>]/DMF series. Numeric ratios indicate the mixed solvent composition, [C2Mim][N(CN)<sub>2</sub>]:DMF. [C2Mim][N(CN)<sub>2</sub>], 1-ethyl-3-methylimidazolium dicyanamide; CD, circular dichroism; CtsPC, chitosan phenylcarbamate; DMF, *N,N*-dimethylformamide.

handed or left handed, respectively.<sup>1</sup> Synthetically considering the results of both UV–Vis–NIR and optical rotatory dispersion measurements, we can reasonably deduce that CtsPC<sub>3,02</sub>/MxS<sub>4/6</sub> and CtsPC<sub>3,02</sub>/MxS<sub>6/4</sub> formed the left- and right-handed arrangements, respectively, of cholesteric architecture.

The other two series, CtsPC<sub>2,72</sub>/MxS and CtsPC<sub>3,51</sub>/MxS lyotropics, were also examined for their chiroptical characteristics in the same technical way described above. For the CtsPC<sub>3,51</sub>/MxS series,

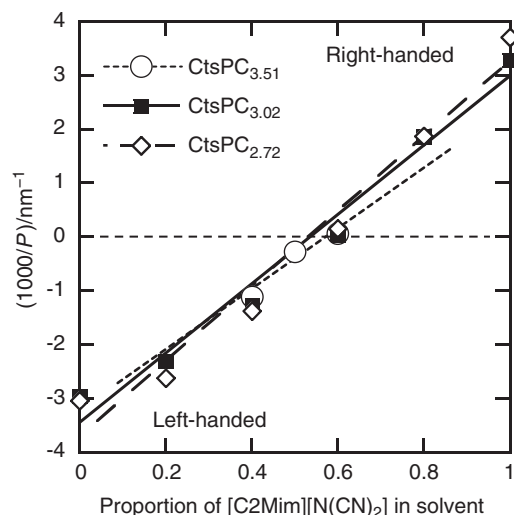


**Figure 11** Plots of  $1000/P$  as a function of solvent composition for three lyotropic series of 46 wt% CtsPC (degrees of substitution (DS) = 2.72, 3.02 and 3.51) in the mixed solvent  $[C2Mim][N(CN)_2]/DMF$  (25 °C). Positive and negative signs of  $P$  indicate the right- and left-handed cholesteric senses, respectively, and  $P^{-1} = 0$  corresponds to a nematic state of the mesophase.  $[C2Mim][N(CN)_2]$ , 1-ethyl-3-methylimidazolium dicyanamide; CtsPC, chitosan phenylcarbamate; DMF, *N,N*-dimethylformamide.

$P$  (as pseudoscalar) was quantified only for three compositions of  $[C2Mim][N(CN)_2]:DMF = 4:6, 5:5$  and  $6:4$  because CtsPC<sub>3.51</sub> powder was not completely soluble in  $[C2Mim][N(CN)_2]$ -rich MxS at the prescribed concentration of 46 wt%, and the use of DMF-rich MxS resulted in gelation of the mixture. However, it was fully confirmed that both the additional two series formed a left- or right-handed cholesteric structure, the handedness depending on the solvent composition in a manner similar to that observed for the CtsPC<sub>3.02</sub>/MxS series. To our knowledge, this report is the first example of conversion of mesoscopic chirality realized by regulating solvent composition, as far as chitin or chitosan derivatives are concerned. However, such a compensation phenomenon of cholesteric pitch using a solvent mixture has been reported for polypeptide lyotropic liquid crystals<sup>30–32</sup> and discussed in terms of the relative dielectric constants of solvent and solute molecules.<sup>30,33</sup> The result of the present work could serve as useful experimental data for future studies, including theoretical or computational analyses of the liquid-crystalline and molecular structures of polysaccharide derivatives.

In Figure 11,  $P^{-1}$  is plotted against the proportion of  $[C2Mim][N(CN)_2]$  in the MxS for the three CtsPC/MxS series. As observed in the figure, the value of  $P^{-1}$  increased almost linearly with increasing  $[C2Mim][N(CN)_2]$  content, and the helical sense inverted at nearly the same fraction (nematic point) of  $[C2Mim][N(CN)_2] \approx 0.55$ , irrespective of the variation in DS of CtsPC. Furthermore, the slope of the regression line for the CtsPC<sub>2.72</sub> series was slightly steeper than that for the CtsPC<sub>3.02</sub> series. This careful observation may be rationalized by a common finding for both the single-solvent systems of CtsPC cholesterics; the absolute value of  $|P|$  increased with increasing DS, despite the solvent used,  $[C2Mim][N(CN)_2]$  or DME. Thus, in the  $P^{-1}$  versus  $[C2Mim][N(CN)_2]$  fraction plots for the mixed-solvent system, the data position would shift upward at  $[C2Mim][N(CN)_2] = 0$  and downward at  $[C2Mim][N(CN)_2] = 1$ , with the increase in DS of the CtsPC sample used. This behavior is responsible not only directly for

the difference in inclination between the regression lines but also secondarily for the smaller shift of the nematic point against the varying DS value.

## CONCLUSIONS

An IL,  $[C2Mim][N(CN)_2]$ , was found to be a novel solvent for highly substituted CtsPC (DS = 2.35–3.51), and the lyotropic system formed a cholesteric mesophase at polymer concentrations exceeding 30 wt%. The mesophase showed a negative concentration dependence, positive temperature dependence and positive DS dependence of supra-molecular helical pitch, and accordingly imparted a variety of colorations because of the selective reflection of visible light. These variations in cholesteric periodicity with multiple dependencies, due to the responsiveness of twist angle (major factor) and distance (rather minor factor) between adjacent nematic layers, were sufficiently characterized by UV-Vis-NIR and CD spectroscopy and X-ray diffractometry. Worthy of special remark is the finding that the CtsPC cholesterics of DS  $\approx 2.8$  (MS  $\approx 3.0$ ) showed high pitch sensitivity, which was sharply changeable, responding to any of the variations in polymer concentration, temperature and DS itself.

Within the limits of the present exploration, the CtsPC/ $[C2Mim][N(CN)_2]$  mesophase retained a right-handed helical structure, although CtsPC was previously known to provide a left-handed cholesteric phase in polar aprotic solvents of DMF, DMAc and dimethyl sulfoxide. As a result of our natural attempt, inversion of the cholesteric sense was achieved by the combined use of  $[C2Mim][N(CN)_2]$  and DME. Regardless of the DS value (*ca.* 2.7–3.5) of the tested CtsPC, an increase of the IL content in the MxS was attended by handedness conversion from left to right in the chiral supramolecular arrangement, together with a prediction of the nematic state of  $P^{-1} = 0$  at an intermediate proportion such as  $[C2Mim][N(CN)_2]:DMF \approx 0.55:0.45$ .

The CtsPC lyotropic system containing an IL component may be significant for practical applications because ILs could respond diversely to external electric perturbations. For example, the present system, either with or without supplementary modification, is potentially functional as a display material under an adequate field of electric force; a disproportionate cation/anion dislocation may induce a dynamic change in cholesteric coloration. Moreover, a unique anisotropic ion conduction could be realized by using the chirality-adjustable layered structure in the mixed-solvent system of CtsPC cholesterics.

## CONFLICT OF INTEREST

The authors declare no conflict of interest.

- Guo, J.-X. & Gray, D. G. in *Cellulosic Polymers, Blends and Composites* (ed. Gilbert, R. D.) Ch. 2. (Hanser, New York, NY, USA, 1994).
- Gray, D. G. & Harkness, B. R. in *Liquid Crystalline and Mesomorphic Polymers* (eds. Shibaev, V. P. & Lam, L.) 298–323 (Springer, New York, NY, USA, 1994).
- Revol, J.-F., Bradford, H., Giasson, J., Marchessault, R. H. & Gray, D. G. Helicoidal self-ordering of cellulose microfibrils in aqueous suspension. *Int. J. Biol. Macromol.* **14**, 170–172 (1992).
- Fukuda, T., Takada, A. & Miyamoto, T. in *Cellulosic Polymers, Blends and Composites* (ed. Gilbert, R. D.) Ch. 3. (Hanser, New York, NY, USA, 1994).
- Zugenmaier, P. in *Cellulosic Polymers, Blends and Composites* (ed. Gilbert, R. D.) Ch. 4. (Hanser, New York, NY, USA, 1994).
- Nishio, Y. Material functionalization of cellulose and related polysaccharides via diverse microcompositions. *Adv. Polym. Sci.* **205**, 97–151 (2006).
- Nishio, Y., Chiba, R., Miyashita, Y., Oshima, K., Miyajima, T., Kimura, N. & Suzuki, H. Salt addition effects on mesophase structure and optical properties of aqueous hydroxypropyl cellulose solutions. *Polym. J.* **34**, 149–157 (2002).



- 8 Chiba, R., Ito, M. & Nishio, Y. Addition effects of imidazolium salts on mesophase structure and optical properties of concentrated hydroxypropyl cellulose aqueous solutions. *Polym. J.* **42**, 232–241 (2010).
- 9 Swatloski, R. P., Spear, S. K., Holbrey, J. D. & Rogers, R. D. Dissolution of cellulose with ionic liquids. *J. Am. Chem. Soc.* **124**, 4974–4975 (2002).
- 10 Rout, D. K., Barman, S. P., Pulapura, S. K. & Gross, R. A. Cholesteric mesophases formed by the modified biological macromolecule 3,6-O-(butyl carbamate)-N-phthaloyl chitosan. *Macromolecules* **27**, 2945–2950 (1994).
- 11 Asahina, D., Miyashita, Y. & Nishio, Y. Synthesis of hydroxypropyl derivatives of chitosan and observation of phase behavior of their aqueous solutions. *Sen'i Gakkaishi* **55**, 28–33 (1999).
- 12 Asahina, D., Matsubara, T., Miyashita, Y. & Nishio, Y. Synthesis of hydroxypropyl derivatives of chitin and chitosan and observation of phase behavior of their aqueous solutions. *Sen'i Gakkaishi* **56**, 435–442 (2000).
- 13 Dong, Y., Yuan, Q., Wu, Y. & Wang, M. Studies on the effect of substitution degree on the liquid crystalline behavior of cyanoethyl chitosan. *J. Appl. Polym. Sci.* **76**, 2057–2061 (2000).
- 14 Revol, J.-F. & Marchessault, R. H. *In vitro* chiral nematic ordering of chitin crystallites. *Int. J. Biol. Macromol.* **15**, 329–335 (1993).
- 15 Gray, D. G. Chiral nematic ordering of polysaccharides. *Carbohydr. Polym.* **25**, 277–284 (1994).
- 16 Kuse, Y., Asahina, D. & Nishio, Y. Molecular structure and liquid-crystalline characteristics of chitosan phenylcarbamate. *Biomacromolecules* **10**, 166–173 (2009).
- 17 Xie, H., Zhang, S. & Li, S. Chitin and chitosan dissolved in ionic liquids as reversible sorbents of CO<sub>2</sub>. *Green Chem.* **8**, 630–633 (2006).
- 18 Mantz, R. A., Fox, D. M., Green, J. M. III, Fylstra, P. A., De Long, H. C. & Trulove, P. C. Z. Dissolution of biopolymers using ionic liquids. *Naturforsch. A* **62**, 275–280 (2007).
- 19 Wu, Y., Sasaki, T., Irie, S. & Sakurai, K. A novel biomass–ionic liquid platform for the utilization of native chitin. *Polymer (Guildf)* **49**, 2321–2327 (2008).
- 20 Noda, A., Susan, M. A. B. H., Kudo, K., Mitsushima, S., Hayamizu, K. & Watanabe, M. Brønsted acid–base ionic liquids as proton-conducting nonaqueous electrolytes. *J. Phys. Chem. B* **107**, 4024–4033 (2003).
- 21 Yoshio, M., Mukai, T., Kanie, K., Yoshizawa, M., Ohno, H. & Kato, T. Layered ionic liquids: anisotropic ion conduction in new self-organized liquid–crystalline materials. *Adv. Mater.* **14**, 351–354 (2002).
- 22 Yue, Z. & Cowie, J. M. G. Synthesis and characterization of ion conducting cellulose esters with PEO side chains. *Polymer (Guildf)* **43**, 4453–4460 (2002).
- 23 Sato, T., Banno, K., Maruo, T. & Nozu, R. New design for a safe lithium-ion gel polymer battery. *J. Power Sources* **152**, 264–271 (2005).
- 24 Bonhôte, P., Dias, A.-P., Papageorgiou, N., Kalyanasundaram, K. & Grätzel, M. Hydrophobic, highly conductive ambient-temperature molten salts. *Inorg. Chem.* **35**, 1168–1178 (1996).
- 25 MacFarlane, D. R., Forsyth, S. A., Golding, J. & Deacon, G. B. Ionic liquids based on imidazolium, ammonium and pyrrolidinium salts of the dicyanamide anion. *Green Chem.* **4**, 444–448 (2002).
- 26 Huddleston, J. G., Visser, A. E., Reichert, W. M., Willauer, H. D., Broker, G. A. & Rogers, R. D. Characterization and comparison of hydrophilic and hydrophobic room temperature ionic liquids incorporating the imidazolium cation. *Green Chem.* **3**, 156–164 (2001).
- 27 Wu, J., Zhang, J., Zhang, H., He, J., Ren, Q. & Guo, M. Homogeneous acetylation of cellulose in a new ionic liquid. *Biomacromolecules* **5**, 266–268 (2004).
- 28 Branco, L. C., Rosa, J. N., Ramos, J. J. M. & Afonso, C. A. M. Preparation and characterization of new room temperature ionic liquids. *Chem. Eur. J.* **8**, 3671–3677 (2002).
- 29 de Vries, H. Rotatory power and other optical properties of certain liquid crystals. *Acta Crystallogr.* **4**, 219–226 (1951).
- 30 Uematsu, I. & Uematsu, Y. Polypeptide liquid crystals. *Adv. Polym. Sci.* **59**, 37–73 (1984).
- 31 Robinson, C. Liquid–crystalline structures in polypeptide solutions. *Tetrahedron* **13**, 219–234 (1961).
- 32 Duke, R. W., Du Pré, D. B., Hines, W. A. & Samulski, E. T. Poly( $\gamma$ -benzyl L-glutamate) helix–coil transition. Pretransition phenomena in the liquid crystal phase. *J. Am. Chem. Soc.* **98**, 3094–3101 (1976).
- 33 Samulski, T. V. & Samulski, E. T. van der Waals–Lifshitz forces in lyotropic polypeptide liquid crystals. *J. Chem. Phys.* **67**, 824–830 (1977).

Supplementary Information accompanies the paper on Polymer Journal website (<http://www.nature.com/pj>)